11056 *Biochemistry* **2009,** *48,* 11056–11066
DOI: 10.1021/bi901461p

BIOCHEMISTRY
including biophysical chemistry & molecular biology
Article

The GTPase Activity of *Escherichia coli* FtsZ Determines the Magnitude of the FtsZ Polymer Bundling by ZapA *in Vitro*[†]

Tamimount Mohammadi,[‡,⊥] Ginette E. J. Ploeger,[‡] Jolanda Verheul,[‡] Anouskha D. Comvalius,[‡] Ariadna Martos,[§] Carlos Alfonso,[§] Jan van Marle,[∥] Germán Rivas,[§] and Tanneke den Blaauwen*[,‡]

[‡]*Swammerdam Institute for Life Sciences, Molecular Cytology, Science Park 904, 1098 XH Amsterdam, The Netherlands,* [§]*Centro de Investigaciones Biológicas, CSIC, Ramiro de Maeztu 9, E-28040 Madrid, Spain, and* [∥]*Department of Cell Biology and Histology/CMO, Academic Medical Center, University of Amsterdam, Meibergdreef 1, NL-1100 DD Amsterdam, The Netherlands*
[⊥]*Present address: Chemical Biology and Organic Chemistry, Bijvoet Center for Biomolecular Research and Institute of Biomembranes, Utrecht University, Padualaan 8, 3584 CH Utrecht, The Netherlands*

Received August 20, 2009; Revised Manuscript Received September 25, 2009

ABSTRACT: FtsZ polymerizes in a ring-like structure at mid cell to initiate cell division in *Escherichia coli*. The ring is stabilized by a number of proteins among which the widely conserved ZapA protein. Using antibodies against ZapA, we found surprisingly that the cellular concentration of ZapA is approximately equal to that of FtsZ. This raised the question of how the cell can prevent their interaction and thereby the premature stabilization of FtsZ protofilaments in nondividing cells. Therefore, we studied the FtsZ−ZapA interaction at the physiological pH of 7.5 instead of pH 6.5 (the optimal pH for FtsZ polymerization), under conditions that stimulate protofilament formation (5 mM $MgCl_2$) and under conditions that stimulate and stabilize protofilaments (10 mM $MgCl_2$). Using pelleting, light scattering, and GTPase assays, it was found that stabilization and bundling of FtsZ polymers by ZapA was inversely correlated to the GTPase activity of FtsZ. As GTP hydrolysis is the rate-limiting factor for depolymerization of FtsZ, we propose that ZapA will only enhance the cooperativity of polymer association during the transition from helical filament to mid cell ring and will not stabilize the short single protofilaments in the cytoplasm. All thus far published *in vitro* data on the interaction between FtsZ and ZapA have been obtained with His-ZapA. We found that in our case the presence of a His tag fused to ZapA prevented the protein to complement a Δ*zapA* strain *in vivo* and that it affected the interaction between FtsZ and ZapA *in vitro*.

FtsZ, ubiquitous in virtually all prokaryotes, is a major actor in the cytokinesis process of bacteria. In *Escherichia coli* this universally conserved tubulin homologue is able to polymerize into a ring-like structure (known as the Z-ring) at the impending site of division. This cytoskeletal element is not only crucial for bacterial cell division but is also required for assembly of other constituents of the divisome (*1*). The ring-like structure is highly dynamic and tightly regulated (*2*, *3*). A number of proteins are involved in the regulation and stability of the Z-ring at mid cell. These regulators are expected to affect the transition from assembly to disassembly and vice versa of the Z-ring. The FtsZ level of 5 μM in the cell (*4*−*6*) is sufficient to promote polymerization as the critical concentration for FtsZ polymerization is in the order of 2 μM (*7*). To avoid the production of mini cells due to polar constrictions, the Min system inhibits FtsZ polymerization near the cell poles (*2*, *8*), and the nucleoid occlusion (Noc) protein SlmA, which is associated with the bacterial chromosome, inhibits FtsZ polymerization in the vicinity of the nucleoid (*9*). As a result FtsZ can only polymerize at mid cell where a local DNA minimum is realized due to segregation of the nucleoids. ZipA, FtsA, and the widely conserved Z-ring associated protein ZapA are reported to stabilize the Z-ring during its formation.

FtsZ is able to bind and hydrolyze GTP (*10*), and its polymerization has been extensively studied in *E. coli*. Assembly of FtsZ into polymers is dependent on GTP hydrolysis (*11*). Association of two FtsZ monomers induces hydrolysis of the interface-bound GTP (*12*), which is followed by a release of the phosphate (*13*, *14*). The remaining GDP-bound FtsZ favors depolymerization (*15*). Depending on experimental conditions, FtsZ can form a variety of polymeric structures. Alterations in concentrations of, for example, FtsZ, GTP, KCl, Mg^{2+}, and Ca^{2+} can affect the polymerization process and result in distinct morphologies of the polymers (*7*, *16*−*19*). Particularly, Mg^{2+} is required for the hydrolysis of GTP as it binds the β- and γ-phosphate. At Mg^{2+} levels between 1 and 5 mM the GTPase activity of FtsZ was demonstrated to be enhanced, resulting in the formation of protofilaments (*7*, *20*−*22*). Above 5 mM (e.g., 10 mM) Mg^{2+} the GTPase activity is reduced, and the filaments are more stable, which results often in enhanced lateral association (*18*, *23*, *24*) and Figures 6 and 8 of this report. Other divalent cations such as Ca^{2+} and DEAE-dextran are not required for assembly but induced lateral associations of protofilaments in very large bundles.

[†]This work was supported by a Vernieuwingsimpuls grant from The Netherlands Organization for Scientific Research (NWO) (016.001.024; T.d.B. and G.E.J.P.) and Grant BIO2008-04478-C03-03 COMBACT_CM S-BIO-0260/2006 (G.R.). This work was funded in part by European Framework Programs COBRA LSHM-CT-2003-503335 (G.E.J.P.) and DIVINOCELL HEALTH-F3-2009-223431 (T.d.B. and G.R.). A.M. is a predoctoral fellow from the Ministerio de Ciencia e Innovación of Spain.

*To whom correspondence should be addressed. Phone: +31-205255196. Fax: +31-205256271. E-mail: t.denblaauwen@uva.nl.

 Published on Web 10/20/2009

Up to now, most studies reported on the effect of *E. coli* ZapA (12.594 kDa) on FtsZ polymerization were carried out at the nonphysiological pH of 6.5 (*25*) as this is the more optimal pH for FtsZ polymerization (*7*, *26*). Under these conditions His-ZapA strongly promotes the bundling of FtsZ and prevents the disassembly of these bundles on a time scale that surpasses the duration of a bacterial cell cycle (*25*). This seems to be in conflict with the very dynamic nature of the Z-ring (*3*). Therefore, we determined the stoichiometry of FtsZ and ZapA *in vivo* and the interaction with FtsZ *in vitro* at pH 7.5 and 6.5 and discovered that the His tag had a substantial effect, questioning previous studies done without removing the His tag (*25*, *27*, *28*).

EXPERIMENTAL PROCEDURES

Materials and Strains. Purified proteins were dialyzed against the buffers used in the experiments. High ionic strength buffer was comprised of 50 mM Tris-HCl, pH 7.5, 500 mM KCl, and 5 mM $MgCl_2$. Low ionic strength buffer contained 50 mM Tris-HCl, pH 7.5, 50 mM KCl, and 5 mM $MgCl_2$ and was used to study the effect of ionic strength on the association state of ZapA. MES buffer, pH 6.5, and HEPES buffer, pH 7.5, contained 50 mM buffering agent and 50 mM KCl. In all experiments 5 or 10 mM $MgCl_2$ was used as indicated. The *E. coli* LMC500 (*29*, *30*) and SF100 (*31*) wild-type strains were grown in minimal medium GB1 or rich medium TY as described (*32*).

Purification of FtsZ. FtsZ was overproduced in *E. coli* BL21(DE3) transformed with pRRE6 and purified as described (*33*). Protein concentration was determined by BCA assay, following the manufacturer's protocol (Pierce, micro BCA kit). The measured concentration of FtsZ was multiplied by 1.23 to correct for the weaker staining of FtsZ compared to BSA[1] by the kit.

Purification of ZapA and Production of Polyclonal Antiserum against ZapA. The *zapA* gene was PCR amplified with the sense primer ZapANcoIFw (5′-CATGCCATGG GGTCTGCACA ACCCGTCGAT ATCC-3′) and the antisense primer ZapA*Sal*IRv (5′-ACGCGTCGAC CATCATTCAA AGTTTTGGTT AGTTTTTTC-3′). The PCR fragment was digested with *Nco*I and *Sal*I and ligated into vector pET302 (*33*) cleaved with the same enzymes. The resulting plasmid pPG016 encodes a C-terminal six histidine tag followed by an enterokinase recognition site (four aspartic acid residues, a lysine, and an alanine residue) fused to the *zapA* gene.

For the purification of ZapA, SF100 cells transformed with pGP016 were grown at 37 °C in TY, and at an OD_{600} of 0.6 overexpression of the recombinant protein was induced by addition of 0.3 mM IPTG. The cultures were then grown for another 2 h after which the cells were harvested by centrifugation. The cell pellet was resuspended in three volumes of ice-cold binding buffer (20 mM phosphate, pH 7.4, 150 mM NaCl, 30 mM imidazole) to which DNase I (20 μg/mL), dithiothreitol (1 mM), and protease inhibitors (0.4 mM Pefabloc plus and complete protease inhibitors (Roche, Germany)) were added. This suspension was passed twice through a French press at 10000 psi, after which unbroken cells were removed by centrifugation (5 min, 12000*g*, 4 °C, SS34 rotor, Sorvall). After ultracentrifugation at 144000*g* for 45 min (Sorvall Discovery 100 centrifuge, Ti60 rotor, 4 °C), glycerol was added to the supernatant to a final concentration of 10%. His-ZapA was then purified in batch by incubating 5 mL of Ni^{2+}-NTA beads (Amersham, Germany) with the supernatant for 1 h at 4 °C under rotation. After washing three times with 10 mL of binding buffer and one time with buffer containing 100 mM imidazole, 6His-ZapA was eluted in 5 times 5 mL elution buffer (20 mM phosphate, pH 7.4, 150 mM NaCl, 500 mM imidazole, 10% glycerol). The eluted fractions were pooled, and the protein concentration was determined using a protein determination kit (micro BCA kit; Pierce) according to the manufacturer's protocol. Antisera against 6His-ZapA were generated using a 1:1 with montenide-diluted 0.1 mg/mL protein solution, which was injected into rabbits (Agrisera, Sweden).

Removal of the His Tag by Enterokinase Digestion of His-ZapA. The His tag of ZapA was removed from His-ZapA in HEPES buffer, pH 7.5, and from His-ZapA in MES buffer, pH 6.5, by digestion with 0.2 and 0.6 μg of enterokinase (Roche), respectively, per 25 μg of ZapA for 21 h at 37 °C. Subsequently, the enterokinase was removed by filtration through a 100-kDA cutoff filter (Microcon YM-100000 MWCO; Millipore). The flow-through was next concentrated by centrifugation through a 10-kDa cutoff filter (Amicon ultra-4 10000 MWCO; Millipore) that removed the His tag. Complete digestion of ZapA and removal of unwanted protein parts was confirmed by SDS−PAGE, and the concentration of the protein was determined by BCA or by Quant-iT assay (Invitrogen). Enterokinase cleaves after the lysine, which results in a ZapA with an extra alanine at its N-terminus.

Quantification of Cellular Concentration of ZapA and FtsZ. LMC500 cells were grown to steady state in GB1 at 28 °C. The number of cells per milliliter was determined using an electronic particle counter (orifice 30 μm). When the ratio between optical density and number of cells remained constant, the culture was considered to be in steady state of growth (*34*). At an OD_{450} of 0.2, the cells were harvested, and to determine the amount of endogenous ZapA or FtsZ per cell, 40 or 67 μL of cell lysate of OD_{450} 0.2 was applied in duplicate or triplicate on a 15% or 12% SDS−PAGE, respectively. Purified FtsZ or ZapA, of which the exact concentration was determined by amino acid quantification (Eurosequence, The Netherlands), was used to make a calibration curve and applied in duplicate on the same SDS−PAGE. The gel was blotted on nitrocellulose, and the blot was incubated with affinity-purified IgG against ZapA or monoclonal antibody F168-12 against FtsZ (*35*) as the primary antibodies and horseradish peroxidase-conjugated goat anti-rabbit or anti-mouse (Bio-Rad) as the secondary antibodies. The blot was then developed with a chemiluminescence kit (ECL plus, Amersham, Germany), followed by quantitative detection of the chemiluminescence signal with a phosphorimager (Storm 840, Amersham, Germany) and analyzed with the program Image J.

Sedimentation Velocity. The experiments were carried out at 42000 rpm and at 20 °C in an XL-I analytical ultracentrifuge (Beckman-Coulter Inc.) equipped with a UV−vis and IF detection system, an An-50 Ti rotor, and 12 mm double-sector centerpieces. Sedimentation profiles were registered every 5 min at the appropriate wavelength (230 or 275 nm). The sedimentation coefficient distributions were calculated by least-squares boundary modeling of sedimentation velocity data using the *c*(*s*) method as implemented in the SEDFIT program (*36*). These *s*-values were corrected to standard conditions (water, 20 °C, and

[1]Abbreviations: BSA, bovine serum albumin; CBB, Coomassie Brilliant Blue; EM, electron microscopy; IPTG, isopropyl β-D-1-thiogalactopyranoside; SDS−PAGE, sodium dodecyl sulfate−polyacrylamide gel electrophoresis.

infinite dilution) to get the corresponding standard *s*-values ($s_{20,w}$) using the software SEDNTERP (*37*). f/f_0 was calculated with this software from the $s_{20,w}$ and the tetramer molecular mass. Mass distributions from the sedimentation velocity experiments were calculated using the *c*(M) maximum entropy routine in SEDFIT (*36*).

Static Light Scattering. Composition-gradient static light-scattering experiments were carried out following essentially the procedure recently developed by Minton and co-workers (*38*). In brief, a programmable three injector-syringe pump (CALYPSO; Wyatt Technology, Santa Barbara, CA) was used to introduce a solution of defined protein composition (loading His-ZapA concentration = 0.4 mg/mL) into parallel flow cells to allow for simultaneous measurement of Rayleigh light scattering at 690 nm and 18 angles (using a DAWN-EOS multiangle laser light scattering detector; Wyatt Technology, Santa Barbara, CA) and protein concentration at 280 nm (using a Spectra System UV2000 absorbance detector; Thermo Finnegan, West Palm Beach, FL). The experiment yields several thousand values of the Rayleigh ratio as a function of protein(s) concentration and scattering angle. The entire composition and angular dependence data can be analyzed in the context of association models as described (*39*) to obtain the average molecular weight and state of association of ZapA under given experimental conditions.

Pelleting Assay. Samples were prepared in HEPES buffer, pH 7.5, or MES buffer, pH 6.5, at 30 °C containing 10 μM FtsZ. Next, ZapA or His-ZapA was added to each sample at various concentrations ranging from 0 to 32 μM (ZapA) or 40 μM (His-ZapA). The polymerization was initiated by the addition of 1 mM GTP. The samples were incubated for 120 s at 30 °C and then centrifuged for 5 min at 178000*g* at 20 °C (Airfuge A100; Beckman-Coulter Inc.). The supernatant (150 μL) was removed, sample buffer was added, and the samples were boiled for 5 min. The pellet was resolved in 100 μL of sample buffer and heated for 10 min at 65 °C before the sample was transferred to an Eppendorf tube and boiled for 5 min. An equal volume of the supernatant and pellet was applied on a 15% SDS−PAGE, and the amount of FtsZ and ZapA present in the pellet and supernatant was determined by densitometry of the CBB stained bands using the program Image J. The data were corrected for the difference in total amount of material applied on the gel of the supernatant and the pellet.

90° Light Scattering for Polymerization Studies. A right-angled (90°) light scattering assay, based on the method described previously by Mukherjee and Lutkenhaus (*7*), was used to study the polymerization of purified FtsZ. In general, light scattering was measured in a PTI QuantaMaster 2000-4 fluorescence spectrophotometer (Photon Technology International, New York) using a quartz cuvette that was maintained at 30 °C by a circulating water bath. In all assays both excitation and emission wavelengths were set at 350 nm with a slit width of 1 or 2 nm. For the standard polymerization assay, ZapA or His-ZapA and/or FtsZ were incubated (in the cuvette) at 30 °C in polymerization buffer in a total volume of 1.3 mL. After establishing a baseline for 2 min, polymerization was induced by addition of 0.2 μM GTP to the reaction mixture. The sample was gently mixed with a pipet tip, and light scattering was monitored for an additional 18−25 min. Data were collected every second, and light scattering following GTP addition was plotted as a function of time. The concentrations and the constituents of the polymerization reaction are indicated in the text and figure legends.

Electron Microscopy. For visualization of the FtsZ polymers by EM, 8.3 μM FtsZ was prewarmed in polymerization buffer (50 mM HEPES, pH 7.5, 50 mM KCl, and 5 or 10 mM $MgCl_2$) at 30 °C. Polymerization was induced by addition of 0.2 mM GTP. After 15 s samples of 3 μL were withdrawn from the polymerization reaction and applied on a 400-mesh carbon-coated grid (EMS, Hatfield, PA), and excess liquid was blotted off. The grid was stained for 1 min with 1 μL of 1% uranyl acetate in water and blotted off again. Subsequently, the grids were dried for 1 h at 30 °C. Grids were examined with a Technai G^2 transmission electron microscope (FEI, Oregon).

GTPase Activity Assay. GTPase activity was assayed by a fluorescence-based assay for phosphate release (*39*). In addition to polymerization buffer (see above) the reaction consisted of 1 mM 7-methylguanosine (excitation at 300 nm), 0.3 unit/mL nucleoside phosphorylase, 8.3 μM FtsZ, and ZapA or His-ZapA at the indicated concentrations in a total volume of 1.3 mL. After recording a baseline for 2 min, polymerization was induced by addition of 0.2 mM GTP. Release of phosphate from GTP hydrolysis was measured by decrease in fluorescence at 390 nm. Standard curves with known concentrations of phosphate were used to convert the decrease in fluorescence to phosphate production.

RESULTS

ZapA Concentration in the E. coli Cell Is Approximately Equimolar to That of FtsZ. To establish conditions that could reflect the cellular situation, we determined the amount of ZapA present in the *E. coli* cell. The ZapA concentration in *Bacillus subtilis* was estimated to be about 5% of the FtsZ concentration in this organism (*28*). Given the large difference in DivIB (FtsQ) function and concentration in *B. subitilis* compared to *E. coli* (*40*), we decided to determine the ZapA concentration in *E. coli* cells. Although the number of FtsZ molecules per cell is well-known, the average number of FtsZ molecules per cell was determined as well to have an internal control for the reliability of our quantification method. In addition, we would be able to directly compare the cellular ZapA concentration with that of FtsZ in cells grown under identical conditions. To this purpose, LMC500 cells were grown to steady state in GB1 at 28 °C. A cell lysate and a purified ZapA concentration range (1−4 ng) were applied in duplicate on SDS−PAGE and subsequently blotted on nitrocellulose (Figure 1). In the case of FtsZ, a 10−100 ng range of purified FtsZ was used as a standard (data not shown). The protein bands were visualized using affinity-purified antibodies against ZapA or FtsZ, and their intensities were determined by chemiluminescence density analysis. By comparing the total signal of the ZapA or FtsZ bands from the cell lysate to that of the standards, the average number of ZapA molecules was calculated to be 6100 ± 1000 per average cell (which equals 5.38 μM or 67.76 μg/mL) as deduced from the average of three separate experiments. This is clearly different from *B. subtilis* ZapA for which the number of molecules per cell was estimated to be 250 (*28*). Note that throughout this report the ZapA concentrations are expressed as that of the monomer. The number of FtsZ molecules per average *E. coli* cell was 4800 ± 1300 as was determined from three separate experiments (results not shown). This is in agreement with the earlier published values for FtsZ of 5000 molecules per cell under comparable growth conditions (*4*), 3200 molecules per cell in *E. coli* B/r (*5*), and 5000 molecules per cell found in *B. subtilis* (*6*). This suggests that in

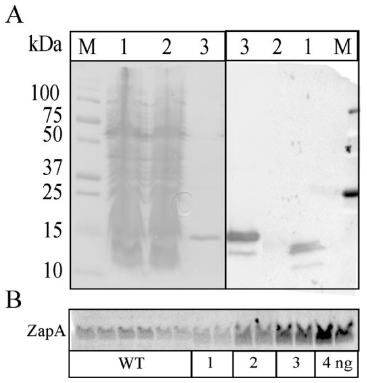

FIGURE 1: Affinity-purified antibodies against ZapA are specific (A) and can be used to quantify the number of ZapA molecules per cell (B). Panel A: The wild-type strain LMC500 (lane 1) and the ZapA null strain LMC3143 (lane 2) were grown in TY at 28 °C and harvested at OD_{600} of 0.5. The cell pellet was resuspended in sample buffer and protease inhibitors, and 2.7 OD units was applied on the gel. On lane 3 1 μg of purified ZapA was applied. The left panel shows a Ponceau staining of the blot, and the right image shows staining with the affinity-purified IgG against ZapA. Panel B: Cell lysates of GB1 at 28 °C grown cells of known cell number and known amounts of purified ZapA were run on gel, immunoblotted, and stained with antibodies against ZapA. Using a phosphorimager, the amount of ZapA in each cell lysate sample could be quantified. WT is LMC500 cell lysate. Endogenous ZapA was found to be present at 6100 ± 1000 molecules per average cell.

E. coli at least during growth in minimal medium ZapA and FtsZ are present in approximately 1:1 stoichiometry.

Characterization of His-ZapA. The crystal structure of *Pseudomonas aeruginosa* His-ZapA showed two His-ZapA dimers associating via an extensive C-terminal coiled-coil protrusion to form an antiparallel tetramer (*27*). Previous analytical ultracentrifugation studies of His-ZapA performed by Small et al. (*25*) were compatible with *E. coli* ZapA being an equilibrium mixture of dimers and tetramers. Much higher concentrations were required to obtain similar results with the His-ZapA of *P. aeruginosa* (*27*). Because ZapA is a rather small protein of molecular mass 12500 Da, the addition of six histidine residues and the enterokinase recognition site of four aspartic acids, a lysine, and an alanine could affect the tetramerization and function of ZapA. Therefore, we first established whether the protein still behaved as wild-type protein *in vivo* and *in vitro*. To this end we determined the oligomeric state of His-ZapA by sedimentation velocity and composition-gradient static light scattering (CG-SLS). We analyzed the sedimentation velocity profiles in terms of distribution of sedimentation coefficients, allowing an evaluation of protein homogeneity and self-association. Figure 2A shows sedimentation velocity data for 40 μM His-ZapA samples equilibrated in buffer of pH 7.5 to mimic the cellular pH of *E. coli* (*41*, *42*) containing 50 mM KCl and 5 mM $MgCl_2$ (solid line). We observed that the major species (> 95%) sediment with a standard *s*-value of 3.4 ± 0.2 S. The sedimentation velocity of the protein did not change upon increasing the salt concentration to 0.5 M KCl or by chelating the magnesium with EDTA (Figure 2A). Based on the *c*(M) distribution (insert in Figure 2A), the molecular mass of His-ZapA was estimated to be 55 ± 0.5 kDa, which is compatible with the expected mass of the protein tetramer (molecular weight of the His-ZapA monomer is 14273). To further measure the molecular mass of the 3.4 S protein species, we carried out in parallel composition-gradient static light scattering experiments. The normalized scattering intensity of His-ZapA in buffer, pH 7.5, with 0.5 M KCl and

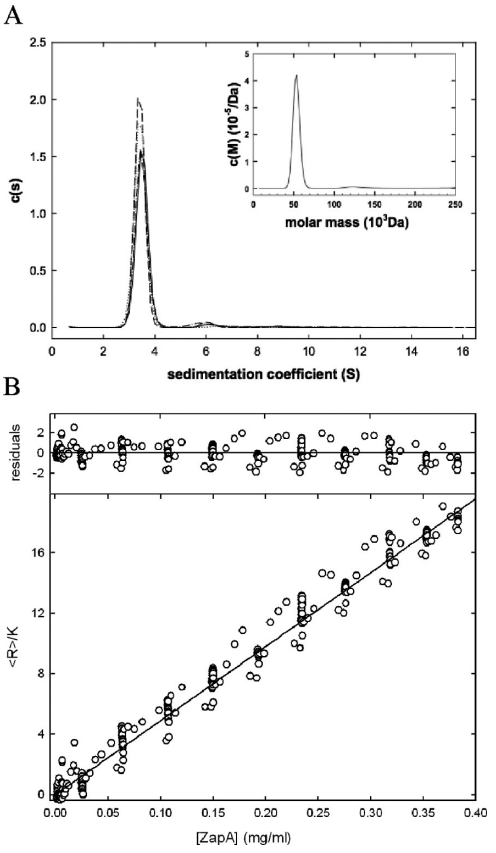

FIGURE 2: Biophysical analysis of His-ZapA in solution. Panel A: Sedimentation coefficient distributions *c*(s) of ~40 μM His-ZapA that result from the analysis of the corresponding sedimentation velocity profiles measured at 42000 rpm and 20 °C with protein equilibrated in 50 mM Tris-HCl buffer, pH 7.5, containing either 0.05 M KCl (solid line, 5 mM $MgCl_2$; dashed-dotted line, EDTA) or 0.5 M KCl (dotted line, 5 mM $MgCl_2$; dashed line, EDTA). The inset shows the corresponding molar mass distribution *c*(M) versus *M*. Panel B: Normalized scattering intensity plotted as a function of His-ZapA concentration in Tris buffer, pH 7.4, containing 0.5 M KCl and 5 mM $MgCl_2$. The solid line is the best fit of a single species model with *M* = 52 ± 0.3 kDa that is compatible with the mass of the His-ZapA tetramer.

5 mM $MgCl_2$ is plotted as a function of protein concentration in Figure 2B. The data have been fitted quantitatively by a model according to which His-ZapA behaves as a single species with an average molecular mass of 52 ± 0.3 kDa (95% confidence limit) in very good agreement with the value obtained from the *c*(M) distribution. The best fit of this model is plotted together with the data set. It follows that under the experimental conditions used His-ZapA is a tetramer species that slightly deviates from the hydrodynamic behavior of a globular protein (frictional ratio $f/f_0 = 1.42$).

His-ZapA Is Not Functional. Although the His-ZapA formed a tetramer as reported for the other His-ZapA proteins (*25*, *27*, *28*), the tag might still interfere with the binding to FtsZ. Therefore, we determined whether our His-ZapA was able to complement a *zapA* deletion strain. Despite the published absence of phenotype of a ZapA deletion mutant strain (*3*, *28*, *43*), during exponential growth in rich medium a minor phenotype could be detected in our *zapA* deletion strain. Consistently, the Δ*zapA* cultures contained a mixture of filaments (11% of the cells) and normal sized cells. The average length of the cells in the culture was 4.9 ± 1.9 μm whereas the average length of cells in a wild-type culture is 3.7 ± 0.8 μm. Based on a Kolmorov−Smirnov

test the two populations are clearly different ($D_{n,n'}$ = 30%, $D_{critical}$ = 6.4%, n = 500 by a 95% confidence limit). We used this morphological difference to determine whether the His-ZapA could replace the ZapA protein. The Δ*zapA* strain LMC3143 was transformed with the plasmid pGP016 that expresses the His-ZapA, with plasmid pGP021 that expresses ZapA without His tag, or with the parental plasmid pTHV037 (*44*) of pGP021 that does not express any protein. The cells were exponentially grown in rich medium at 28 °C. The average length of the cells in these cultures was 4.6 ± 1.7, 3.1 ± 1.0, and 4.6 ± 2.8 μm, respectively, indicating that the His-ZapA is not functional *in vivo*.

Interaction of ZapA and FtsZ under Physiological Relevant Conditions. *In vitro* studies on the interaction of ZapA and FtsZ showed that ZapA very strongly stabilizes and stimulates bundling of FtsZ polymers (*25*). The surprisingly high concentration of ZapA in the *E. coli* cells, given the reported 250 molecules of ZapA in *B. subtilis* cells (*28*), made us wonder how *E. coli* can prevent ZapA to prematurely stabilize and bundle FtsZ polymers in the cytosol before they are needed to assemble the Z-ring. Recently, it was shown that ZapA is able to prevent the FtsZ polymerization inhibitory activity of MinC (*45*, *46*). Thus, MinC might prevent the stabilization of FtsZ polymers by ZapA. However, ZapA is present throughout the cytosol, whereas the Min system is thought to be predominantly functional in the cell poles. Therefore, additional mechanisms might be needed to prevent premature interaction between ZapA and FtsZ. To understand how ZapA might interact with FtsZ in nondividing cells and with the Z-ring in dividing cells, we performed the experiments at the physiological pH of 7.5 (*41*). To check for consistency with published data (*25*) the experiments were also performed at pH 6.5. In addition, it was attempted to assay their interaction under conditions that do not stimulate bundling (to mimic predivision conditions) and conditions under which FtsZ filaments were already somewhat stabilized (to mimic Z-ring formation). The first condition was assessed by measuring polymerization in the presence of 5 mM $MgCl_2$ (*7*, *20*−*22*). The second condition was in the presence of 10 mM $MgCl_2$ that reduces the GTPase activity of FtsZ (*7*). We removed the His tag because we found that it did not complement the ZapA null strain. Information on the behavior of the His-ZapA in the below described assays can be found in the Supporting Information and figures.

Using a pelleting assay (*25*, *27*, *47*, *48*), we found that ZapA stoichiometrically pelleted FtsZ in the presence of 10 mM $MgCl_2$ at pH 7.5 (Figure 3A) as well as at pH 6.5 (Figure 3B; see for all corresponding SDS−PAGE gels Supporting Information Figure S1). In contrast, in the presence of 5 mM $MgCl_2$ at pH 7.5, ZapA did not pellet FtsZ (Figure 3A), whereas at pH 6.5 FtsZ was still pelleted by ZapA albeit less efficiently (Figure 3B). In conclusion, the efficiency of FtsZ pelleting decreased in the following order: pH 6.5, 10 mM $MgCl_2$ > pH 7.5, 10 mM $MgCl_2$ > pH 6.5, 5 mM $MgCl_2$ > pH 7.5, 5 mM $MgCl_2$. The ability of ZapA to pellet FtsZ was most markedly stimulated by 10 mM $MgCl_2$. (See for the behavior of His-ZapA Supporting Information Figure S2.) The predivision mimicking condition clearly resulted in a difference in FtsZ−ZapA interaction than the Z-ring mimicking condition.

Light Scattering Experiments. To obtain further insight in the nature of the differences in the stabilization of FtsZ by ZapA and to be able to follow the polymerization and the depolymerization process, we repeated the experiments by measuring light scattering. No increase in light scattering signal was seen when either 1 mM GDP replaced GTP or no guanosines were employed as reported (*25*). A light scattering signal increase was also absent when ZapA was assayed in the absence of FtsZ (Supporting Information Figure S3). With 5 mM $MgCl_2$ and in the presence of a substoichiometric to stoichiometric ZapA concentration, the light scattering signal showed a small increase (Figure 4 and Supporting Information Figure S4; see for His-ZapA data Supporting Information Figure S5). This might indicate that ZapA binds to protofilaments and causes an augmentation in the amount of scattered light due to the increased thickness of the filaments or due to a change in the length of the filaments (see EM data below). In the presence of 10 mM $MgCl_2$ the light scattering signal increased much more (Figure 4). At pH 7.5 the polymers started to depolymerize within the time course of the experiment (Figure 4A). However, at pH 6.5 the light scattering signal was completely stable within the time span of the experiment (Figure 4B). To verify that the FtsZ polymers were able to depolymerize at pH 6.5 in the presence of 10 mM $MgCl_2$, the experiment was repeated with 0.03 mM GTP instead of 0.2 mM GTP as was used in the above experiments. Under these conditions depolymerization of FtsZ occurred within the time span of the experiment (Figure 5), which meant that with a molar ratio of FtsZ to GTP of 1:3 a considerable amount of polymers was still formed in the presence

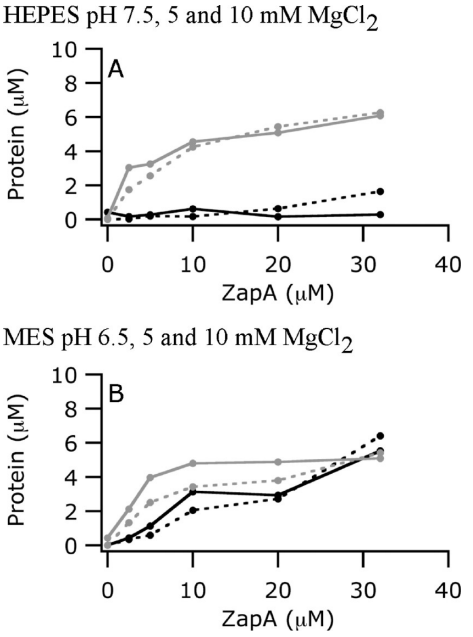

FIGURE 3: Quantification of the proteins in a pelleting assay shows that ZapA precipitates FtsZ effectively in the presence of 10 mM $MgCl_2$ and to a much lesser extent in the presence of 5 mM $MgCl_2$. FtsZ (10 μM) was incubated in prewarmed MES buffer, pH 6.5, or HEPES buffer, pH 7.5, of 30 °C with increasing ZapA concentrations. Polymerization was initiated by the addition of 1 mM GTP and allowed to continue for 2 min before the polymers were pelleted by airfuge. Supernatant and the pellet were applied on a 15% SDS−PAGE, which was stained with CBB. The stained gel was imaged, and the amount of material present in the supernatant and the pellet was determined by densitometry. The protein concentration was plotted as a function of the ZapA concentration added to the sample. Panel A: Quantification of the pellets of the CBB stained gels of the experiments in HEPES buffer, pH 7.5. Panel B: Quantification of the pellets of the experiment in MES buffer, pH 6.5. Solid lines are from the FtsZ in the pellet and dashed lines from the ZapA in the pellet. Black and gray lines are from the experiments in the presence of 5 and 10 mM $MgCl_2$, respectively. The corresponding CBB stained gels are shown in Supporting Information Figure S1.

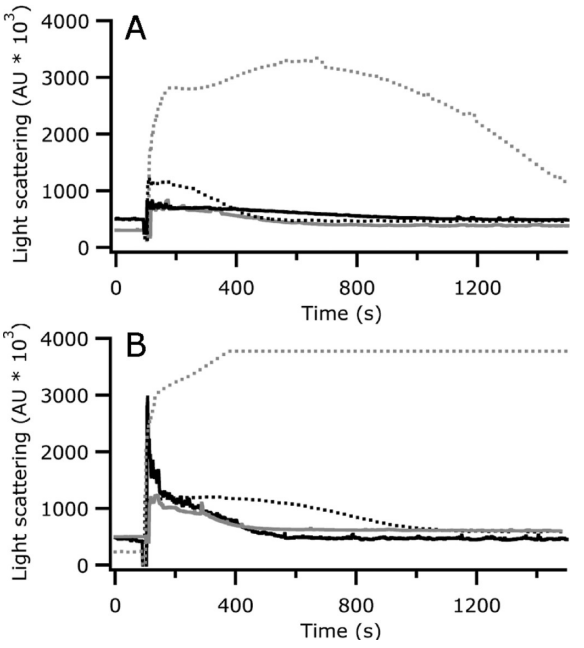

FIGURE 4: Light scattering analysis shows that ZapA stimulates FtsZ polymer bundling in the presence of 10 mM $MgCl_2$ but not in the presence of 5 mM $MgCl_2$. Polymerization of 8.3 μM FtsZ in HEPES buffer, pH 7.5 (A), or in MES buffer, pH 6.5 (B), at 30 °C. At pH 7.5 and 10 mM $MgCl_2$ the bundles are much less stable (panel A) whereas at pH 6.5 and 10 mM $MgCl_2$ the bundles are extremely stable (panel B). Traces: gray dotted, 10 mM $MgCl_2$ and 4.1 μM ZapA; black dotted, 5 mM $MgCl_2$ and 4.1 μM ZapA; gray solid, 10 mM $MgCl_2$ and no ZapA; black solid, 5 mM $MgCl_2$ and no ZapA. Polymerization was initiated by the addition of 0.2 mM GTP.

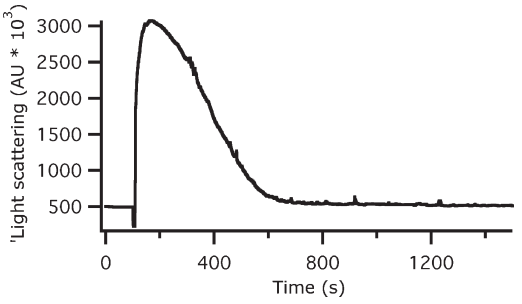

FIGURE 5: Light scattering of FtsZ polymerization (8.3 μM) in MES buffer, pH 6.5, and 10 mM $MgCl_2$ induced with 0.03 mM GTP at 30 °C in the presence of 2 μM ZapA. The polymers are able to depolymerize within 1200 s in this buffer if the GTP concentration is reduced from 0.2 to 0.03 mM.

of ZapA. FtsZ polymers are normally very transient in the absence of an excess of GTP because of the high rate of GTP turnover by FtsZ (*26*). These results suggested, therefore, that ZapA considerably stabilized the polymers by decreasing the GTPase activity of FtsZ or by simply cross-linking the polymers (see below).

GTPase Activity Assays. To verify whether the GTPase activity of FtsZ was indeed affected by ZapA, we determined its GTPase activity in the presence of ZapA under the same conditions as used for the light scattering assays. A fluorescent molecule 7-methylguanosine that is converted to a nonfluorescent molecule by purine nucleoside phosphorylase was used to monitor the phosphate release due to the GTP hydrolyzing activity of FtsZ. First, the GTPase activity of 8.3 μM FtsZ in the absence of ZapA was measured under the four conditions used: pH 6.5, pH 7.5, and 5 or 10 mM $MgCl_2$. The lowering of the

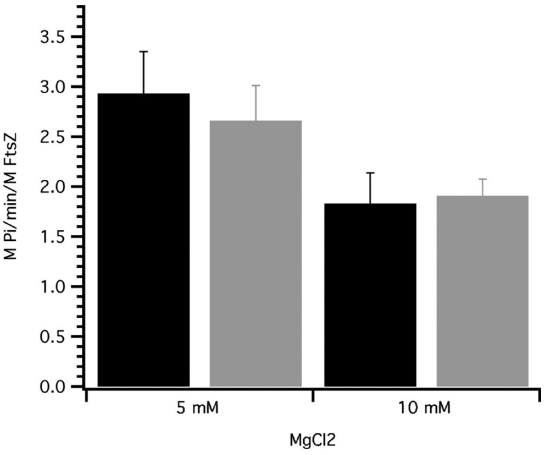

FIGURE 6: GTPase activity of 8.3 μM FtsZ in HEPES buffer, pH 7.5 (black), or MES buffer, pH 6.5 (gray), in the presence of 5 or 10 mM $MgCl_2$ as indicated. The data show the average of five experiments. The phosphate release was measured using 0.2 mM 7-methylguanosine as fluorescent marker (excitation at 300 nm) and 0.3 unit/mL purine nucleoside phosphorylase (PNP). After recording a baseline for several minutes, polymerization was induced by addition of 0.2 mM GTP. Release of phosphate from GTP hydrolysis was measured by the decrease in fluorescence at 390 nm. The determination of the initial velocity of the reaction was based on the slopes obtained by linear regression of the experimental data of the first 100−150 s. Using the same buffer conditions, a range of phosphate concentrations was used to calibrate the GTPase activity.

pH gave a small decrease in the GTPase activity of FtsZ, whereas the addition of 10 mM instead of 5 mM $MgCl_2$ caused a decrease in GTPase activity of 30% (Figure 6). Subsequently, the GTPase activity of 8.3 μM FtsZ was measured using the same four buffer conditions in the presence of ZapA or His-ZapA (Supporting Information Figure S7) in concentrations ranging from 1 to 8.3 μM. The resulting GTPase activities are plotted as a percentage of the FtsZ GTPase activity in the absence of ZapA (Figure 7). Overall, it seems that up to a stoichiometric concentration of 8.3 μM, ZapA had little effect on the GTPase activity of FtsZ in the presence of 5 mM $MgCl_2$, confirming its lack of effect on the polymers in general under these conditions. In the presence of 10 mM $MgCl_2$ the GTPase activity was slightly inhibited up to 20% at the highest ZapA concentration used. It should be noted that FtsZ polymers are already stabilized at much lower ZapA concentration in the light scattering experiments (not shown) and pelleting experiments (Figure 2) in the presence of 10 mM $MgCl_2$. ZapA concentrations at which no effect on the GTPase activity of FtsZ is observed. Lateral association of FtsZ protofilaments is known to decrease the GTPase activity of FtsZ, which consequently stabilizes the bundles (*7*). The weak effect of ZapA on the GTPase activity of FtsZ in combination with its strong stabilizing effect suggests that ZapA does not actively reduce the GTPase activity of FtsZ and that the observed mild decrease in GTPase activity might be just the consequence of the lateral association of FtsZ protofilaments.

Morphology of FtsZ−ZapA Polymers. A possible explanation for the lack of effect of ZapA on the FtsZ polymer stability in the presence of 5 mM $MgCl_2$ could be that ZapA simply does not bind or has a very low affinity for protofilaments. In contrast, the presence of 10 mM $MgCl_2$ and its accompanying reduced GTPase activity of FtsZ might stimulate bundling of protofilaments. This would provide a binding site for which ZapA could have a much higher affinity. To verify this hypothesis, the morphology of the filaments was studied by electron microscopy

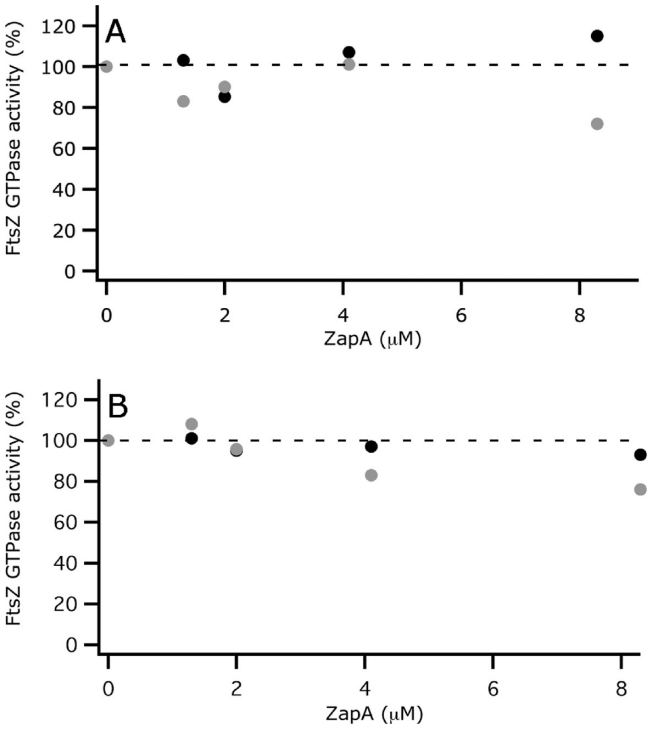

FIGURE 7: ZapA seems not to affect the GTPase activity of FtsZ dramatically. FtsZ (8.3 μM) was preincubated with various ZapA concentrations at 30 °C in HEPES buffer, pH 7.5 (A), or in MES buffer, pH 6.5 (B), in the presence of 5 mM $MgCl_2$ (black markers) or 10 mM $MgCl_2$ (gray markers), with 0.2 mM 7-methylguanosine (excitation at 300 nm) and 0.3 unit/mL PNP. After recording a baseline for several minutes, polymerization was induced by addition of 0.2 mM GTP. Release of phosphate from GTP hydrolysis was measured by the decrease in fluorescence at 390 nm. The initial velocity of the reaction was fitted by linear regression as described in the legend of Figure 6, and the slope was plotted on the *Y*-axis as percentage of the activity of FtsZ in the absence of ZapA obtained from Figure 6.

(EM) using the same experimental conditions as described for the light scattering and GTPase activity measurements. Samples were applied on an EM grid 15 s after addition of GTP that initiated the polymerization reaction in HEPES, pH 7.5, buffer. In the presence of 5 mM $MgCl_2$ FtsZ forms predominantly short protofilaments and thin bundles of protofilaments (thickness of the filamentous structures was 11.4 ± 3.9, n = 57; Figure 8A). In the presence of 10 mM $MgCl_2$ the filaments seemed to be longer but not thicker (thickness of the filamentous structures was 11.5 ± 3.0, n = 88; Figure 8B). Addition of ZapA in the presence of 5 mM $MgCl_2$ did not cause an obvious change in the structure of the filaments (thickness 11.3 ± 4.1, n = 156; Figure 8C), whereas bundles of protofilaments are observed in the presence of 10 mM $MgCl_2$. They often appeared as regular arrays of parallel filaments separated with an interprotofilament distance (distance between two adjacent FtsZ filaments) of 22.1 ± 4.1 nm, n = 110 (Figure 8D and enlargement in Figure 8E). If the tetrameric ZapA (MW 50 kDa) would bind to the FtsZ (45 kDa) protofilaments, one would expect the filaments in the presence of 5 mM $MgCl_2$ to become slightly thicker because of the added mass. However, this is not observed. In the absence of FtsZ, it was not possible to see recognizable ZapA structures on the grids. Therefore, the EM images are not conclusive as to whether ZapA binds to the filaments in the presence of 5 mM $MgCl_2$. Occasionally, about four adjacent filaments similar to those observed in the presence of 10 mM $MgCl_2$ were seen, suggesting that ZapA

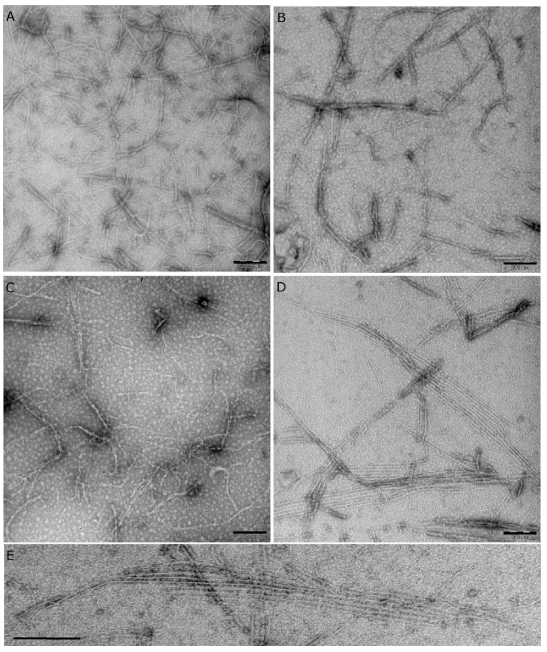

FIGURE 8: Electron microscopy images of uranyl acetate stained FtsZ filaments in the absence and presence of ZapA in 50 mM HEPES, pH 7.5, and 50 mM KCl buffer at 30 °C. The FtsZ concentration was 8.3 μM, and the reaction was initiated with 0.2 mM GTP. After 15 s a sample was removed from the reaction mixture and applied on an EM grid. FtsZ in the presence of 5 and 10 mM $MgCl_2$ (A and B, respectively). FtsZ filaments in the presence of 4.1 μM ZapA and 5 and 10 mM $MgCl_2$ (C and D, respectively). An enlargement of a parallel array of FtsZ filaments from a sample with 4.1 μM ZapA in the presence of 10 mM $MgCl_2$ (E). The bar equals 200 nm.

is in principle able to promote bundling at the lower $MgCl_2$ concentration. The His-ZapA induced arrays of parallel running filaments in the presence of 10 mM $MgCl_2$ with an interfilament distance of 24.8 ± 4.7 nm, n = 88. Interestingly, the filaments bundled by ZapA were almost always double protofilaments (thickness 10.5 ± 3.1 nm, n = 79), whereas the His-ZapA bundled single protofilaments (thickness 6.5 ± 1.7 nm, n = 85) as if the His-ZapA tetramer lacked two binding sites (Figure 9). In conclusion, ZapA seems to arrange double FtsZ protofilaments in a precise conformation.

DISCUSSION

The Cellular Concentration of E. coli FtsZ and ZapA Is Approximately the Same. To obtain a better understanding of the possible role of ZapA during the cell cycle of *E. coli*, we investigated the interaction between ZapA and FtsZ at near physiological conditions. We found that the concentration of the ZapA protein in minimal medium grown bacteria was approximately identical to that of FtsZ (i.e., 5 μM). We could not reconcile this high ZapA concentration in the cell with the published *in vitro* data showing the strong and persistent promotion of FtsZ bundling by ZapA. *In vivo*, FtsZ is always present in the cell at a concentration sufficiently high to polymerize, but the small polymers are continuously depolymerized due to the inhibitory activities of the Min system and the nucleoid occlusion system (*8*, *9*). One would expect ZapA to stabilize these small emerging protofilaments and cause FtsZ to form large precipitates in the cell. This is not what generally is reported in FtsZ localization studies (*49*−*52*). To find out how ZapA discriminates in the cell, which protofilaments should be stabilized, we

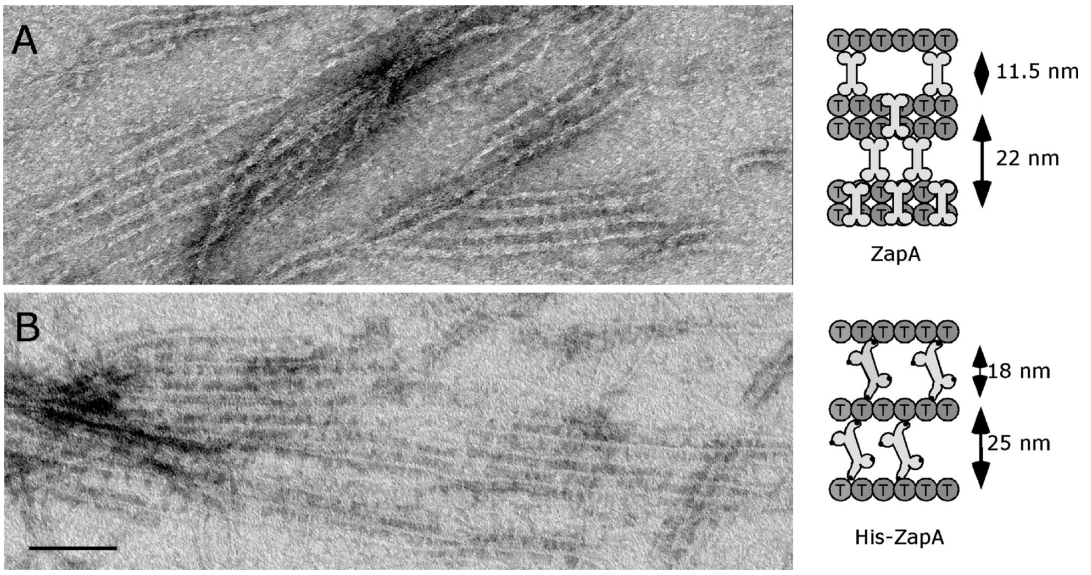

FIGURE 9: Electron microscopy images of uranyl acetate stained FtsZ filaments in the presence of ZapA (A) or His-ZapA (B). The FtsZ concentration was 8.3 μM, and the ZapA or His-ZapA concentration was 4.1 μM. The polymerization was performed in 50 mM HEPES, pH 7.5, 50 mM KCl, and 10 mM $MgCl_2$ at 30 °C and initiated by the addition of 0.2 mM GTP. The bar equals 100 nm. To the right of images A and B a model shows a possible interpretation of the images. ZapA might be able to bind in between FtsZ protofilaments as well as on top of a double filament (A). His-ZapA might not be able to bind on top of double filaments because of steric hindrance due to the presence of the His tag and appears to cover a larger distance between two filaments (B). The gray circles present FtsZ molecules, T is GTP, and the light gray bone-like shape presents the ZapA tetramer and the black dot the His tag.

tried to mimic two conditions. One condition would result in predominantly protofilaments (5 mM $MgCl_2$ (*7*, *20*−*22*)) that would resemble small cytosolic FtsZ filaments in nondividing cells. The second condition would mimic the assemblage of the Z-ring by modestly inhibiting the GTPase activity of FtsZ causing the protofilaments to be more stable and often associate (10 mM $MgCl_2$ (*7*, *24*, *53*)). We decided to study the interaction between ZapA and FtsZ at pH 7.5 because this reflects the pH of the cytosol more closely (*41*, *42*) than pH 6.5, which is more optimal for FtsZ polymerization (*7*, *26*).

The His-ZapA Is Not Functional in Vivo. The His-ZapA appeared not to be functional, as it could not restore the filamentous phenotype of our ZapA deletion strain to normal rod shape whereas expression of ZapA could. In addition, the His tag protein did not pellet FtsZ stochiometrically in the pelleting assay and behaved differently from ZapA in all *in vitro* assays. Therefore, the His tag was removed by enterokinase digestion for all experiments apart from studies on the oligomeric state of ZapA.

Effect of Buffer Composition on the in Vitro Interaction of ZapA and FtsZ. The interaction between FtsZ and ZapA was studied by pelleting, light scattering, and GTPase activity assays. Significant differences in polymer behavior between pH 7.5 and pH 6.5 as well as with the two concentrations of $MgCl_2$ were found.

In all experiments up to stoichiometric concentrations of ZapA had little effect on the polymerization of FtsZ in the presence of 5 mM $MgCl_2$ either at pH 6.5 or at pH 7.5. Under these conditions, FtsZ forms short filaments that are not laterally associated. This suggests that ZapA can only stabilize FtsZ filaments that are already somewhat associated. This is illustrated by the ability of ZapA to bundle FtsZ in the presence of 10 mM $MgCl_2$, which itself stimulates lateral association of FtsZ filaments (*53*). The stoichiometry of the interaction appears to be 1:1 as was found for *P. aeruginosa* His-ZapA (*27*) and *B. subtilis* His-ZapA (*25*). The His-ZapA of Small et al. (*25*) pelleted FtsZ in a 1:2 stoichiometry, and our His-ZapA did not pellet FtsZ in a fixed ratio (Supporting Information Figure S2), suggesting that the His tag in the case of *E. coli* ZapA is more of a hindrance than in the other two organisms.

The presence of 10 mM $MgCl_2$ did reduce the GTPase activity of FtsZ by 30%, causing an increase in the length of the FtsZ polymers but not in the amount of filaments bundling as judged from the electron microscopy images of polymers sampled after 15 s. As the bundling is cooperative, longer incubation times result in more bundling in the presence of 10 mM $MgCl_2$ compared to 5 mM $MgCl_2$ as published (*7*, *53*). The subsequent addition of ZapA did not affect the GTPase activity of FtsZ particularly but caused a considerable change in the morphology of the bundles, which appeared to consist of very orderly parallel-aligned filaments separated by a constant space of 22 nm. Remarkably at pH 7.5, this stabilizing effect was transient whereas at pH 6.5 the stabilization lasted at least 30 min before the light scattering signal began to decrease again. A reduction in the ZapA concentration to 2 μM and the GTP concentration to 30 μM (approximately 1 FtsZ molecule to 3 GTP molecules) was required to observe depolymerization in the time span of the experiment (Figure 5). As the Z-ring is reported to be completely renewed every 18 s (*3*), the extreme stabilization of FtsZ polymers at pH 6.5 cannot reflect, in our opinion, the endogenous situation. Theoretically, ZapA possesses the same charge at pH 6.5 as at pH 7.5, whereas FtsZ has a charge of −18 at pH 6.5 and of −20 at pH 7.5. Overall, this seems to be a small difference, but locally two extra charges can affect the interaction between two proteins. However, it is the GTPase activity that is decreased by the lower pH and by the higher $MgCl_2$ concentration (Figure 6). Because the GTPase activity is the limiting factor in polymer turnover (*14*), the polymers are more stable at pH 6.5 and at 10 mM $MgCl_2$. For the cross-linking of FtsZ protofilaments, ZapA has to bind multiple FtsZ monomers, which makes it plausible that FtsZ polymer stability affects the ZapA binding ability. We could not reproduce the 100% inhibition of the

GTPase activity of FtsZ by His-ZapA as published by Small et al. (*25*). At a 1:1 His-ZapA concentration we find about 40% inhibition (Supporting Information Figure S6). The differences between our data and the data of Small are most likely due to a difference in the His-tagged version of ZapA.

Morphology of the ZapA-Stabilized FtsZ Filaments. On the basis of the crystal structure of *P. aeruginosa* ZapA (*27*) it was anticipated that the amino-terminal His tag was unlikely to interfere with the tetrameric state of ZapA as the carboxy termini are the responsible parts for tetramerization (Supporting Information Figure S7). Using analytical ultracentrifugation and static light scattering, we found that His-ZapA is predominantly a tetramer irrespective of salt levels, pH, or magnesium concentration. The published K_d of 320 nM for His-ZapA determined in MES buffer, pH 6.5, and 10 mM $MgCl_2$ by Small et al. (*25*) and the fact that association of proteins is favored by the macromolecular crowding in the cytoplasm strongly suggest that at the cytosolic concentration of 5 μM all ZapA molecules will be part of a tetramer. The length of the unhydrated tetrameric ZapA molecule, as derived from its crystal structure (*27*), is approximately 10 nm, whereas the distance from the middle of a double FtsZ filament to the next parallel double filament in Figure 9A is 22 ± 4 nm ($n = 110$). If a ZapA tetramer would bind in between them (Figure 9A), the distance to be covered would be 11.5 nm (Figure 9A) and more or less correspond to the length of a ZapA tetramer, which could differ somewhat between *E. coli* and *P. aeruginosa* ZapA. The width of the parallel double FtsZ filaments is about 10.5 ± 3 nm ($n = 79$). Possibly, a ZapA tetramer is also able to bind on top of a double FtsZ filament. Although electron microscopic tomography images show FtsZ filaments as scattered arcs in a *Caulobacter* cell (*54*), a configuration in which FtsZ filaments should be kept segregated by ZapA tetramers seems to be in conflict with the not very essential nature of ZapA. Therefore, the binding in between filaments should more likely have a function in bringing the filaments together, which is supported by the following observations.

The GTPase activity of FtsZ is determined by the pH of the buffer and to a much larger extent by the Mg^{2+} concentration (Figure 6 and ref *26*). A high GTPase activity results in shorter protofilaments than a lower GTPase activity because GTP hydrolysis is the rate-limiting step in polymer depolymerization (*14*). Because of the cooperative nature of the polymerization and of the lateral association of protofilaments (*55*), the protofilaments will more readily bundle at pH 6.5 than at pH 7.5 and still more in the case of 10 mM $MgCl_2$ compared to 5 mM $MgCl_2$. Based on the results of the *in vitro* assays presented in Figures 3 and 4, the magnitude of the FtsZ−ZapA interaction follows the same trend while ZapA affects the GTPase activity of FtsZ itself marginally (Figure 7). This suggests that the presence of lateral interactions between FtsZ polymers stimulates the binding of ZapA and most likely is a requirement for the interaction of ZapA with FtsZ. In the EM images that were collected after 15 s of polymerization (Figures 8 and 9) but also in images obtained after incubation for 30 s or for 5 min (not shown) regular arrays of parallel double FtsZ filaments separated by a fixed width are observed. We speculate that by binding in between the protofilaments ZapA enhances their chance to associate. As the association is cooperative, the filaments will become more stable when they are annealed over a particular length of the filaments making continued action of ZapA superfluous.

ZapA−FtsZ Interaction in Vivo. The MinC protein of the Min system that prevents polar Z-ring formation (*8*) has been reported to prevent lateral association of FtsZ filaments and possibly to compete with ZapA for the same binding site on FtsZ (*45*, *46*). ZapA requires two adjacent FtsZ filaments to stimulate their lateral association, whereas MinC needs only one filament to prevent association. This putative higher affinity of MinC for small protofilaments could prevent ZapA from effectively binding and associating FtsZ polymers near the cell poles. The SlmA protein inhibits Z-ring formation in the vicinity of the nucleoid by a presently unknown mechanism (*9*).

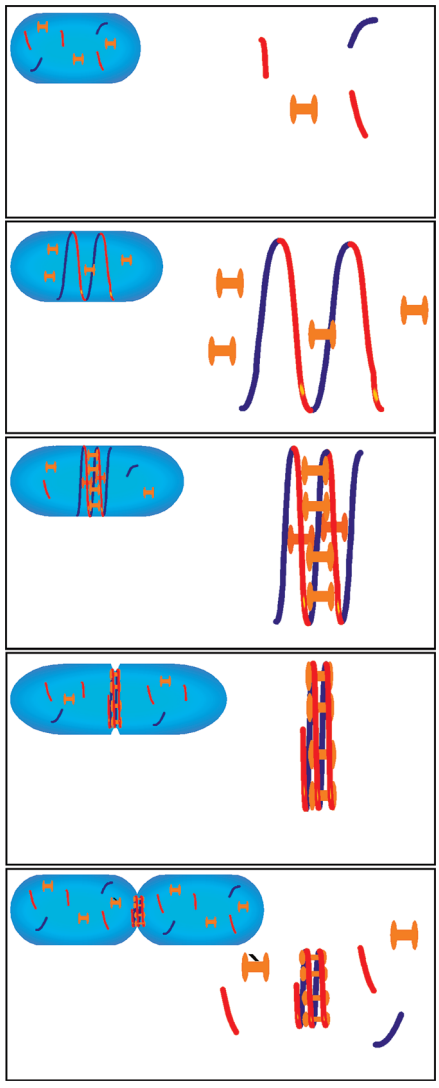

FIGURE 10: Hypothetical model for the interaction between ZapA and FtsZ. From top to bottom: In young cells FtsZ (red and blue) forms continuously short filaments that are destabilized by the Min and nucleoid occlusion systems. At the appropriate length to initiate cell division the inhibition of MinC, which functions predominantly at the cell poles, and of the partly segregated nucleoids is not sufficient any more, and the filaments will become longer, eventually organizing, possibly with the help of FtsA and ZipA (*49*), into a helical structure (*49*, *50*). This structure assembles into the Z-ring. By binding in between the filaments ZapA (orange) increases the chance of lateral association. Once the Z-ring is established, this ZapA activity is not needed anymore, and ZapA will bind at the cytoplasmic side on top of the filaments, where it might have a weak structural function in the association of other cell division proteins. The cells are shown on the left, and an enlargement of the FtsZ polymer−ZapA interaction is shown on the right.

We propose the following model for the interaction of ZapA with FtsZ during the cell cycle (Figure 10). In nondividing cells the MinC and SlmA activity that negatively regulate

polymerization of FtsZ prevent the growth of the FtsZ polymers to a length sufficient to laterally associate. ZapA is not able to bundle single protofilaments, and therefore no FtsZ ring can be initiated despite the presence of ZapA and FtsZ at stoichiometric concentrations. At a specific cell length the MinC and SlmA activity is too low to prevent FtsZ polymers from becoming of sufficient length, and with the help of FtsA and ZipA a helical arrangement of FtsZ polymers is formed underneath the cytoplasmic membrane (*49*, *50*). Especially under conditions of fast growth when less time is available to depend on lateral association by chance only, ZapA will be beneficial to the survival of the cells by bringing the helical FtsZ filaments together and thus assist in the timely formation of the Z-ring. As a result only Δ*zapA* cells grown in rich medium have a phenotype. Once the Z-ring is established, ZapA binds to the ring where it has perhaps a weak structural function in the assembly of the divisome.

ACKNOWLEDGMENT

We thank B. M. Blaauwster for patience and inspiring attitude, L. C. M. Zuiderwijk and N. Nanninga for critically reading the manuscript, and Carmen Fernández-Alonso (CIB, Madrid) for help with preliminary sedimentation velocity analysis. We also thank Henk van Veen for electron microscopy assistance.

SUPPORTING INFORMATION AVAILABLE

Figures showing Coomassie Brilliant Blue stained SDS−PAGE gels corresponding to the graphs in Figure 3 (S1), control light scattering experiments (S3), and light scattering experiments of FtsZ with increasing concentrations of ZapA at pH 7.5 and 5 mM $MgCl_2$ (S4), figures that show the effect of His-ZapA on the polymerization of FtsZ in a pelleting assay (S2) and its effect in a light scattering assay (S5), and figures that illustrate the influence of His-ZapA on the GTPase activity of FtsZ (S6) and the structure of ZapA showing the position of the His tag (S7). This material is available free of charge via the Internet at http://pubs.acs.org.

REFERENCES

1. den Blaauwen, T., de Pedro, M. A., Nguyen-Disteche, M., and Ayala, J. A. (2008) Morphogenesis of rod-shaped sacculi. *FEMS Microbiol. Rev. 32*, 321–344.
2. Harry, E., Monahan, L., and Thompson, L. (2006) Bacterial cell division: the mechanism and its precison. *Int. Rev. Cytol. 253*, 27–94.
3. Anderson, D. E., Gueiros-Filho, F. J., and Erickson, H. P. (2004) Assembly dynamics of FtsZ rings in *Bacillus subtilis* and *Escherichia coli* and effects of FtsZ-regulating proteins. *J. Bacteriol. 186*, 5775–5781.
4. Pla, J., Sanchez, M., Palacios, P., Vicente, M., and Aldea, M. (1991) Preferential cytoplasmic location of FtsZ, a protein essential for *Escherichia coli* septation. *Mol. Microbiol. 5*, 1681–1686.
5. Rueda, S., Vicente, M., and Mingorance, J. (2003) Concentration and assembly of the division ring proteins FtsZ, FtsA, and ZipA during the *Escherichia coli* cell cycle. *J. Bacteriol. 185*, 3344–3351.
6. Feucht, A., and Errington, J. (2005) ftsZ mutations affecting cell division frequency, placement and morphology in *Bacillus subtilis*. *Microbiology 151*, 2053–2064.
7. Mukherjee, A., and Lutkenhaus, J. (1999) Analysis of FtsZ assembly by light scattering and determination of the role of divalent metal cations. *J. Bacteriol. 181*, 823–832.
8. Raskin, D. M., and de Boer, P. A. (1999) Rapid pole-to-pole oscillation of a protein required for directing division to the middle of *Escherichia coli*. *Proc. Natl. Acad. Sci. U.S.A. 96*, 4971–4976.
9. Bernhardt, T. G., and de Boer, P. A. (2005) SlmA, a nucleoid-associated, FtsZ binding protein required for blocking septal ring assembly over chromosomes in *E. coli*. *Mol. Cell 18*, 555–564.
10. Mukherjee, A., Dai, K., and Lutkenhaus, J. (1993) *Escherichia coli* cell division protein FtsZ is a guanine nucleotide binding protein. *Proc. Natl. Acad. Sci. U.S.A. 90*, 1053–1057.
11. Michie, K. A., and Lowe, J. (2006) Dynamic filaments of the bacterial cytoskeleton. *Annu. Re. Biochem. 75*, 467–492.
12. Scheffers, D. J., de Wit, J. G., den Blaauwen, T., and Driessen, A. J. (2002) GTP hydrolysis of cell division protein FtsZ: evidence that the active site is formed by the association of monomers. *Biochemistry 41*, 521–529.
13. Scheffers, D. J., and Driessen, A. J. (2002) Immediate GTP hydrolysis upon FtsZ polymerization. *Mol. Microbiol. 43*, 1517–1521.
14. Romberg, L., and Mitchison, T. J. (2004) Rate-limiting guanosine 5′-triphosphate hydrolysis during nucleotide turnover by FtsZ, a prokaryotic tubulin homologue involved in bacterial cell division. *Biochemistry 43*, 282–288.
15. Romberg, L., and Levin, P. A. (2003) Assembly dynamics of the bacterial cell division protein FtsZ: poised at the edge of stability. *Annu. Rev. Microbiol. 57*, 125–154.
16. Lowe, J., and Amos, L. A. (1999) Tubulin-like protofilaments in Ca^{2+}-induced FtsZ sheets. *EMBO J. 18*, 2364–2371.
17. Yu, X. C., and Margolin, W. (1997) Ca^{2+}-mediated GTP-dependent dynamic assembly of bacterial cell division protein FtsZ into asters and polymer networks in vitro. *EMBO J. 16*, 5455–5463.
18. Rivas, G., Lopez, A., Mingorance, J., Ferrandiz, M. J., Zorrilla, S., Minton, A. P., Vicente, M., and Andreu, J. M. (2000) Magnesium-induced linear self-association of the FtsZ bacterial cell division protein monomer. The primary steps for FtsZ assembly. *J. Biol. Chem. 275*, 11740–11749.
19. Tadros, M., Gonzalez, J. M., Rivas, G., Vicente, M., and Mingorance, J. (2006) Activation of the *Escherichia coli* cell division protein FtsZ by a low-affinity interaction with monovalent cations. *FEBS Lett. 580*, 4941–4946.
20. Popp, D., Iwasa, M., Narita, A., Erickson, H. P., and Maeda, Y. (2009) FtsZ condensates: an *in vitro* electron microscopy study. *Biopolymers 91*, 340–350.
21. Huecas, S., Llorca, O., Boskovic, J., Martin-Benito, J., Valpuesta, J. M., and Andreu, J. M. (2008) Energetics and geometry of FtsZ polymers: nucleated self-assembly of single protofilaments. *Biophys. J. 94*, 1796–1806.
22. Gonzalez, J. M., Velez, M., Jimenez, M., Alfonso, C., Schuck, P., Mingorance, J., Vicente, M., Minton, A. P., and Rivas, G. (2005) Cooperative behavior of *Escherichia coli* cell-division protein FtsZ assembly involves the preferential cyclization of long single-stranded fibrils. *Proc. Natl. Acad. Sci. U.S.A. 102*, 1895–1900.
23. Mukherjee, A., and Lutkenhaus, J. (1998) Dynamic assembly of FtsZ regulated by GTP hydrolysis. *EMBO J. 17*, 462–469.
24. White, E. L., Ross, L. J., Reynolds, R. C., Seitz, L. E., Moore, G. D., and Borhani, D. W. (2000) Slow polymerization of *Mycobacterium tuberculosis* FtsZ. *J. Bacteriol. 182*, 4028–4034.
25. Small, E., Marrington, R., Rodger, A., Scott, D. J., Sloan, K., Roper, D., Dafforn, T. R., and Addinall, S. G. (2007) FtsZ polymer-bundling by the *Escherichia coli* ZapA orthologue, YgfE, involves a conformational change in bound GTP. *J. Mol. Biol. 369*, 210–221.
26. Mendieta, J., Rico, A. I., Lopez-Vinas, E., Vicente, M., Mingorance, J., and Gomez-Puertas, P. (2009) Structural and functional model for ionic (K(+)/Na(+)) and pH dependence of GTPase activity and polymerization of FtsZ, the prokaryotic ortholog of tubulin. *J. Mol. Biol. 390*, 17–25.
27. Low, H. H., Moncrieffe, M. C., and Lowe, J. (2004) The crystal structure of ZapA and its modulation of FtsZ polymerisation. *J. Mol. Biol. 341*, 839–852.
28. Gueiros-Filho, F. J., and Losick, R. (2002) A widely conserved bacterial cell division protein that promotes assembly of the tubulin-like protein FtsZ. *Genes Dev. 16*, 2544–2556.
29. Peters, J. E., Thate, T. E., and Craig, N. L. (2003) Definition of the *Escherichia coli* MC4100 genome by use of a DNA array. *J. Bacteriol. 185*, 2017–2021.
30. Taschner, P. E., Huls, P. G., Pas, E., and Woldringh, C. L. (1988) Division behavior and shape changes in isogenic *ftsZ*, *ftsQ*, *ftsA*, *pbpB*, and *ftsE* cell division mutants of *Escherichia coli* during temperature shift experiments. *J. Bacteriol. 170*, 1533–1540.
31. Baneyx, F., and Georgiou, G. (1990) *In vivo* degradation of secreted fusion proteins by the *Escherichia coli* outer membrane protease OmpT. *J. Bacteriol. 172*, 491–494.
32. Koppelman, C. M., Aarsman, M. E., Postmus, J., Pas, E., Muijsers, A. O., Scheffers, D. J., Nanninga, N., and den Blaauwen, T. (2004) R174 of *Escherichia coli* FtsZ is involved in membrane interaction and protofilament bundling, and is essential for cell division. *Mol. Microbiol. 51*, 645–657.
33. van der Does, C., Manting, E. H., Kaufmann, A., Lutz, M., and Driessen, A. J. (1998) Interaction between SecA and SecYEG in

micellar solution and formation of the membrane-inserted state. *Biochemistry 37*, 201–210.
34. Fishov, I., Zaritsky, A., and Grover, N. B. (1995) On microbial states of growth. *Mol. Microbiol. 15*, 789–794.
35. Voskuil, J. L., Westerbeek, C. A., Wu, C., Kolk, A. H., and Nanninga, N. (1994) Epitope mapping of *Escherichia coli* cell division protein FtsZ with monoclonal antibodies. *J. Bacteriol. 176*, 1886–1893.
36. Schuck, P. (2000) Size-distribution analysis of macromolecules by sedimentation velocity ultracentrifugation and Lamm equation modeling. *Biophys. J. 78*, 1606–1619.
37. Laue, T. M., Shah, B. D., Ridgeway, T. M., and Pelletier, S. L. (1992) Computer-aided interpretation of analytical sedimentation data for proteins, in Analytical Ultracentrifugation in Biochemistry and Polymer Science (Harding, S. E., Rowe, A. J., Horton, J. C., Eds.) The Royal Society of Chemistry, Cambridge, pp 90–125.
38. Attri, A. K., and Minton, A. P. (2005) New methods for measuring macromolecular interactions in solution via static light scattering: basic methodology and application to nonassociating and self-associating proteins. *Anal. Biochem. 337*, 103–110.
39. Läppchen, T., Hartog, A. F., Pinas, V. A., Koomen, G. J., and den Blaauwen, T. (2005) GTP analogue inhibits polymerization and GTPase activity of the bacterial protein FtsZ without affecting its eukaryotic homologue tubulin. *Biochemistry 44*, 7879–7884.
40. Real, G., Autret, S., Harry, E. J., Errington, J., and Henriques, A. O. (2005) Cell division protein DivIB influences the Spo0J/Soj system of chromosome segregation in *Bacillus subtilis*. *Mol. Microbiol. 55*, 349–367.
41. Padan, E., Zilberstein, D., and Schuldiner, S. (1981) pH homeostasis in bacteria. *Biochim. Biophys. Acta 650*, 151–166.
42. Zilberstein, D., Agmon, V., Schuldiner, S., and Padan, E. (1984) *Escherichia coli* intracellular pH, membrane potential, and cell growth. *J. Bacteriol. 158*, 246–252.
43. Johnson, J. E., Lackner, L. L., Hale, C. A., and de Boer, P. A. (2004) ZipA is required for targeting of DMinC/DicB, but not DMinC/MinD, complexes to septal ring assemblies in *Escherichia coli*. *J. Bacteriol. 186*, 2418–2429.
44. Aarsman, M. E., Piette, A., Fraipont, C., Vinkenvleugel, T. M., Nguyen-Disteche, M., and den Blaauwen, T. (2005) Maturation of the *Escherichia coli* divisome occurs in two steps. *Mol. Microbiol. 55*, 1631–1645.
45. Dajkovic, A., Lan, G., Sun, S. X., Wirtz, D., and Lutkenhaus, J. (2008) MinC spatially controls bacterial cytokinesis by antagonizing the scaffolding function of FtsZ. *Curr. Biol. 18*, 235–244.
46. Scheffers, D. J. (2008) The effect of MinC on FtsZ polymerization is pH dependent and can be counteracted by ZapA. *FEBS Lett. 582*, 2601–2608.
47. Scheffers, D., and Driessen, A. J. (2001) The polymerization mechanism of the bacterial cell division protein FtsZ. *FEBS Lett. 506*, 6–10.
48. Romberg, L., Simon, M., and Erickson, H. P. (2001) Polymerization of Ftsz, a bacterial homolog of tubulin, is assembly cooperative? *J. Biol. Chem. 276*, 11743–11753.
49. Peters, P. C., Migocki, M. D., Thoni, C., and Harry, E. J. (2007) A new assembly pathway for the cytokinetic Z ring from a dynamic helical structure in vegetatively growing cells of *Bacillus subtilis*. *Mol. Microbiol. 64*, 487–499.
50. Thanedar, S., and Margolin, W. (2004) FtsZ exhibits rapid movement and oscillation waves in helix-like patterns in *Escherichia coli*. *Curr. Biol. 14*, 1167–1173.
51. Erickson, H. P. (1997) FtsZ, a tubulin homologue in prokaryote cell division. *Trends Cell Biol. 7*, 362–367.
52. den Blaauwen, T., Buddelmeijer, N., Aarsman, M. E. G., Hameete, C. M., and Nanninga, N. (1999) Timing of FtsZ assembly in *Escherichia coli*. *J. Bacteriol. 181*, 5167–5175.
53. Chen, Y., and Erickson, H. P. (2009) FtsZ filament dynamics at steady state: subunit exchange with and without nucleotide hydrolysis. *Biochemistry 48*, 6664–6673.
54. Li, Z., Trimble, M. J., Brun, Y. V., and Jensen, G. J. (2007) The structure of FtsZ filaments in vivo suggests a force-generating role in cell division. *EMBO J. 26*, 4694–4708.
55. Lan, G., Dajkovic, A., Wirtz, D., and Sun, S. X. (2008) Polymerization and bundling kinetics of FtsZ filaments. *Biophys. J. 95*, 4045–4056.